Molecular Therapy
Methods & Clinical Development
Original Article

Immunocompromised Cas9 transgenic mice for rapid *in vivo* assessment of host factors involved in highly pathogenic virus infection

Nicole Collette,[1] Pragyesh Dhungel,[2,4] Sean J. Lund,[2,4] Jennifer L. Schwedler,[2,4] Edwin A. Saada,[3] Yooli K. Light,[3] Anupama Sinha,[3] Joseph S. Schoeniger,[3] and Oscar A. Negrete[2]

[1]Physical and Life Science Directorate, Lawrence Livermore National Laboratory, Livermore, CA, 94550, USA; [2]Department of Biotechnology and Bioengineering, Sandia National Laboratories, Livermore, CA 94550, USA; [3]Department of Systems Biology, Sandia National Laboratories, Livermore, CA 94550, USA

Targeting host factors for anti-viral development offers several potential advantages over traditional countermeasures that include broad-spectrum activity and prevention of resistance. Characterization of host factors in animal models provides strong evidence of their involvement in disease pathogenesis, but the feasibility of performing high-throughput *in vivo* analyses on lists of genes is problematic. To begin addressing the challenges of screening candidate host factors *in vivo*, we combined advances in CRISPR-Cas9 genome editing with an immunocompromised mouse model used to study highly pathogenic viruses. Transgenic mice harboring a constitutively expressed *Cas9* allele (*Cas9*$^{tg/tg}$) with or without knockout of type I interferon receptors served to optimize *in vivo* delivery of CRISPR single-guide RNA (sgRNA) using Invivofectamine 3.0, a simple and easy-to-use lipid nanoparticle reagent. Invivofectamine 3.0-mediated liver-specific editing to remove activity of the critical Ebola virus host factor Niemann-Pick disease type C1 in an average of 74% of liver cells protected immunocompromised *Cas9*$^{tg/tg}$ mice from lethal surrogate Ebola virus infection. We envision that immunocompromised *Cas9*$^{tg/tg}$ mice combined with straightforward sgRNA *in vivo* delivery will enable efficient host factor loss-of-function screening in the liver and other organs to rapidly study their effects on viral pathogenesis and help initiate development of broad-spectrum, host-directed therapies against emerging pathogens.

INTRODUCTION

Animal models of viral infection serve a vital role in pre-clinical countermeasure development. Because reagents and genetic strains are widely available in mice, these small rodents typically serve as a starting point for animal model development of viral infection. For pathogens such as Ebola virus (EBOV), use of immunocompromised mice is necessary for productive pathogenic infection with wild-type or primary virus isolates.[1,2] The type I interferon knockout (*Ifnar1*$^{-/-}$) mouse model, which lacks expression of the interferon (IFN)-α/β receptors, is immunocompromised and, thus, more susceptible to infection by many highly pathogenic viruses, including filoviruses, flaviviruses, alphaviruses, bunyaviruses, and henipaviruses .[3,4] Because the *Ifnar1*$^{-/-}$ mouse is susceptible to a range of emerging viruses of public health concern, this model can serve as a powerful platform for early *in vivo* screening of medical countermeasures.

Traditional therapeutic agents directly targeting the pathogen of interest face issues of rapid emergence of resistance and lack of broad-spectrum activity against multiple pathogens or variants. Host-directed therapeutic agents, on the other hand, which target the host cellular proteins required for infection, offer alternative strategies against emerging viruses with the advantage of broad-range utility in targeting common cellular pathways used by multiple viruses. It follows that regulation of such host genes will be less susceptible to incurring resistance.[5] Characterization of host factors in animal models provides strong evidence of their involvement in human disease pathogenesis, but it has been proven difficult to perform *in vivo* analyses on comprehensive lists of target genes.[6,7] With the advent of genome editing technologies via CRISPR-mediated engineering,[8] *in vivo* host factor target validation may become more efficient and high throughput than previously possible if optimized CRISPR delivery platforms are developed for broad applicability and can be formulated with speed and ease.[9–11]

We set out to optimize the simple and easy-to-use lipid nanoparticle (LNP) reagent Invivofectamine 3.0 (INVFT3.0) for CRISPR applications in mice. INVFT3.0 is a proprietary LNP reagent originally designed for liver-targeted delivery of small interfering RNA (siRNA) in mice via systemic administration[12]. Given the relative similarities in mass sizes between CRISPR single-guide RNA (sgRNA) (32 kDa) and siRNA (15 kDa), we reasoned that sgRNA delivery into *Cas9*$^{tg/tg}$ mice using INVFT3.0 for rapid characterization of host factors in animal models was feasible. As a proof-of-concept study, sgRNAs were designed to efficiently target the critical EBOV

Received 23 April 2021; accepted 24 September 2021;
https://doi.org/10.1016/j.omtm.2021.09.012.

[4]These authors contributed equally

Correspondence: Oscar Negrete, PhD, Sandia National Laboratories, PO Box 969, MS 9292, Livermore, CA 94551, USA.
E-mail: onegret@sandia.gov

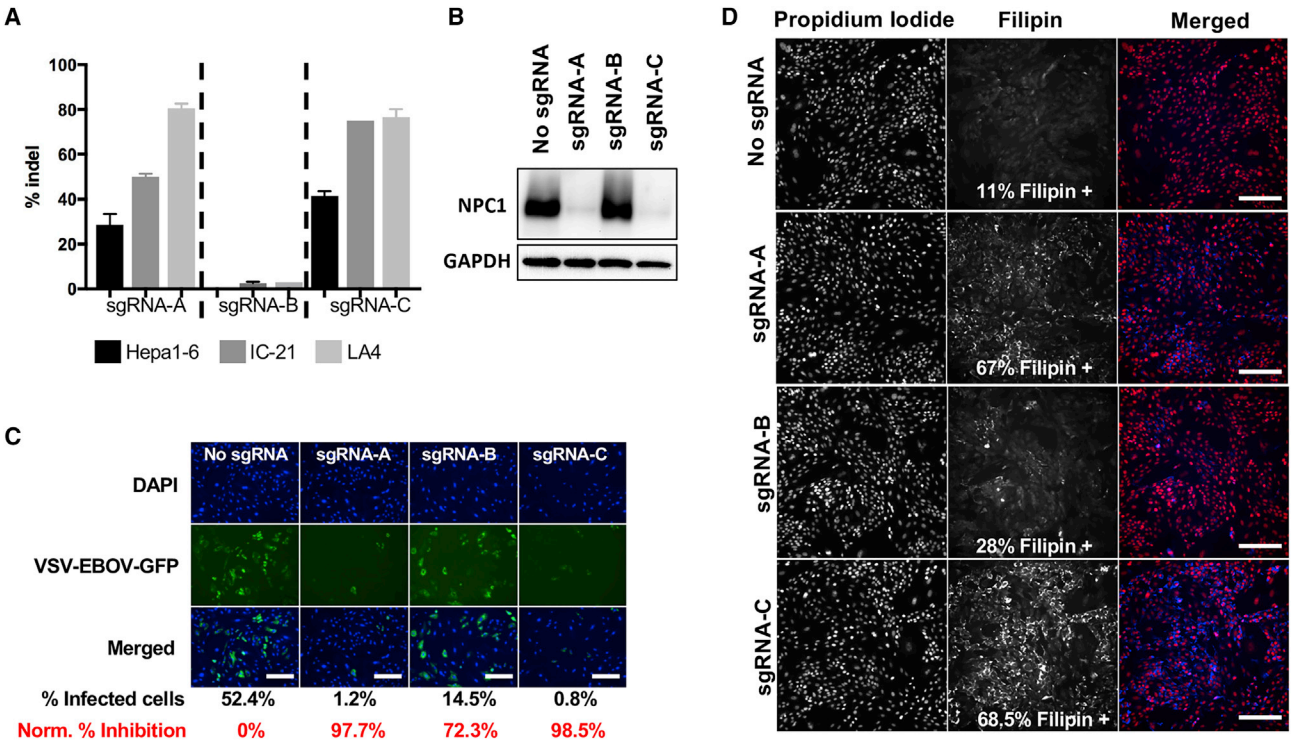

Figure 1. Screening *Npc1*-targeting sgRNAs in mouse cell lines for *in vitro* efficacy

(A) Three sgRNAs targeting mouse *Npc1* were evaluated in three mouse cell lines. Percent indels were calculated based on duplicate RNP transfection per sgRNA and per cell type. Data are depicted as mean + standard deviation. (B) Cell lysates from LA4 RNP-transfected cells were subjected to western blot analysis using NPC1 and Glyceraldehyde 3-phosphate dehydrogenase (GAPDH) antibodies. (C) RNP-transfected LA4 cells were infected with VSV-EBOV-GFP at 1 MOI, analyzed at 18 hpi for percent infection and normalized as percent inhibition (red text) (see also Figure S1). Representative infection levels are shown as images of nucleus staining (DAPI, blue) and VSV-EBOV-GFP (green) separately or merged. (D) Similarly, RNP-transfected LA4 cells were analyzed for cholesterol accumulation using filipin and PI nucleus staining; representative images are shown. Percent filipin-positive cells was analyzed using cell cytometry. Scale bars, 300 μM.

host factor gene Niemann-Pick disease type C1 (*Npc1*)[13] to generate a loss-of-function (LOF) allele. Npc1 is an endo/lysosomal membrane protein involved in intracellular cholesterol trafficking, and its luminal domain C is an essential endosomal receptor for Ebola and Marburg filoviruses.[14] Moreover, Npc1 is a critical host factor in general for the filoviruses because bat-derived filovirus strains also utilize this receptor to gain entry into cells.[13,15,16] These findings suggest that Npc1 might be an interesting broad-spectrum therapeutic target of filovirus infection.

To further understand the role of Npc1 in EBOV disease progression, we utilized $Cas9^{tg/tg}$ mice and those crossed with knockout of type I IFN receptors ($Cas9^{tg/tg}$; $Ifnar1^{-/-}$) to optimize *in vivo* delivery of sgRNA targeting mouse *Npc1* using INVFT3.0. Additionally, a replication-competent pseudovirus based on vesicular stomatitis virus (VSV) encoding the Ebola glycoprotein (VSV-EBOV) that mimics authentic EBOV cell entry[16] was used for development of an infection model in $Cas9^{tg/tg}$; $Ifnar1^{-/-}$ mice. We report the parameters required for efficient *in vivo* genome editing in $Cas9^{tg/tg}$ and $Cas9^{tg/tg}$; $Ifnar1^{-/-}$ mice using INVFT3.0. We further highlight a partial knockout phenotype resulting from liver-specific *Npc1* LOF editing in immunocompromised $Cas9^{tg/tg}$ mice as being completely protective against lethal VSV-EBOV challenge.

RESULTS

Screening Npc1 sgRNAs in mouse cell lines identifies a target sequence for *in vivo* evaluation

To achieve efficient *in vivo* editing using CRISPR genome engineering, sgRNAs were first screened *in vitro*. Three sgRNA sequences targeting the mouse *Npc1* locus were designed using publicly available algorithms (Figure S1A) and labeled in Figure 1 as sgRNA-A, sgRNA-B, and sgRNA-C. These three top-ranking sgRNA designs were synthesized and assembled as CRISPR ribonucleoprotein (RNP) complexes for transfection into mouse-derived LA4 (lung epithelial), Hepa1-6 (hepatoma), and IC-21 (macrophage) cells. As shown in Figure 1A, 2 of 3 sgRNA designs efficiently edited *Npc1* 4 days after transfection with sgRNA-C, resulting in the highest percentage of insertions or deletions (indels) in all three cell types (77% LA4, 42% Hepa1-6, and 75% IC-21) compared with the other two sequences. *Npc1*-edited LA4 cells were then selected for phenotypic analysis, given their advantages over Hepa1-6 and IC-21 cells in terms of level of editing, susceptibility to infection, and characterization by

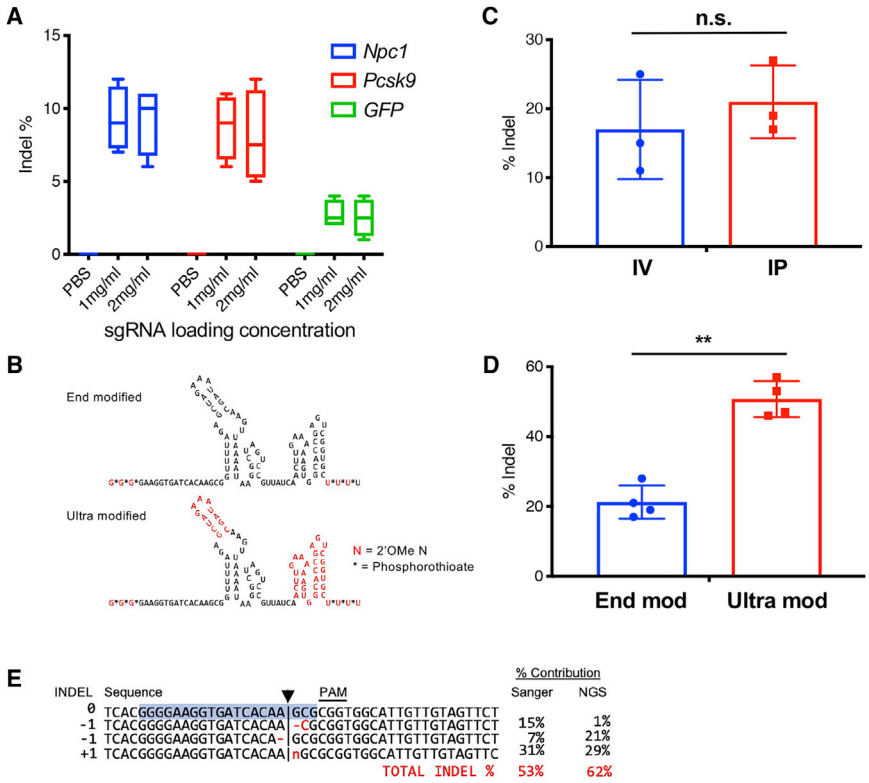

Figure 2. Optimization of sgRNA *in vivo* delivery to the liver of *Cas9* transgenic mice using INVFT3.0

(A) INVFT3.0-based LNPs were loaded with standard end-modified sgRNAs targeting mouse *Npc1*, *Pcsk9*, or *GFP* using the modified manufacturer's instructions described for siRNA. sgRNA loading concentrations of 1 mg/mL or 2 mg/mL were used and tested. LNP formulations were administered i.v. to *Cas9* mice, and editing at the *Npc1*, *Pcsk9*, or *GFP* locus of the liver was analyzed on day 7 after dosing (4 mice per group). (B) End- versus ultra-modified sgRNA chemical compositions. (C) Performance of ultra-modified *Npc1* sgRNA-loaded INVFT3.0 LNPs was evaluated by comparing i.v. and i.p. injections at a dose of 0.75 mg/kg (sgRNA wt/mouse wt). (D) Direct editing efficiency comparison of end- or ultra-modified sgRNAs targeting *Npc1* was performed via i.p. administration at a dose of 1.5 mg/kg. (E) Percent indels is reported based on decomposition of chromatographs from Sanger sequencing using Synthego ICE, and a comparison with indel sequences and percentages based on amplicon sequencing using NGS is shown for a single sample. Data are depicted as mean ± standard deviation. Not significant (ns), $p > 0.1$; **$p < 0.001$.

image-based assays. Western blotting demonstrated that sgRNA-A and sgRNA-C-mediated *Npc1* LOF reduced protein to undetectable levels compared with controls (Figure 1B). Additionally, VSV-EBOV expressing green fluorescent protein (GFP) (VSV-EBOV-GFP) was used to infect RNP-transfected LA4 cells, and again sgRNA-A and sgRNA-C were highly potent because they reduced the number of infected GFP-expressing cells by approximately 98% when normalized to the control (no sgRNA) condition (Figures 1C and S1B). Last, knockout of the cholesterol transporter function of Npc1 resulted in intracellular cholesterol accumulation that was visualized through filipin staining. Filipin is an antibiotic isolated from *Streptomyces filipinensis* that is used for diagnosis of Niemann-Pick type C disease and binds to unesterified cholesterol, resulting in a fluorescence shift. Treatment with RNPs containing either sgRNA-A or sgRNA-C resulted in 67-68% cholesterol accumulation in LA4 cells compared to 11% in the control transfection condition as observed via filipin staining (Figure 1D). Interestingly, sgRNA-A and sgRNA-C *Npc1* targeting sequences mapped to exon 11 and were spaced only 3 nt apart, whereas sgRNA-B mapped to exon 10 (Figure S1B), suggesting that exon 11 may be more accessible for CRISPR-Cas9 genome editing than exon 10 (Figure S1C). Based on the sum of the *in vitro* efficacy data, sgRNA-C was selected for *in vivo* characterization because of its high level of editing in all cell types tested, which resulted in efficient *Npc1* LOF indel formation, protein reduction, phenotypic loss of cholesterol transport function, and elimination of the EBOV receptor that protected cells from infection by VSV-EBOV-GFP.

Ultra-modified sgRNAs are highly efficient at editing the liver of Cas9 transgenic mice using INVFT3.0

To start, mouse *Npc1* sgRNA-C selected from *in vitro* screening experiments (now referred to as *Npc1* sgRNA) was encapsulated into INVFT3.0 LNPs using a protocol slightly modified from that described for siRNA (Materials and methods). In parallel, we also composed INVFT3.0 LNPs with a published sgRNA sequence targeting the endogenous proprotein convertase subtilisin/kexin type 9 (*Pcsk9*), which is also expressed in liver cells, and knockout leads to lipid and cholesterol accumulation in the liver.[17] As an additional control, we targeted *GFP* because *Cas9*$^{tg/tg}$ mice express a *Cas9-GFP* fusion transcript.[18] Instead of using the 2.4 mg/mL starting siRNA concentration recommended by the manufacturer for loading INVFT3.0 LNPs, 1 mg/mL or 2 mg/mL sgRNA loading concentrations were used. LNP formulations and PBS mock controls were administered to Cas9 mice via intravenous (i.v.) dosing, and editing at the *Npc1*, *Pcsk9*, or *GFP* locus of the mouse liver was analyzed on day 7 after dosing (Figure 2A). Although an average of 2%–9% editing was seen under all evaluated conditions (*Npc1*, 9.3% ± 2.1%; *Pcsk9*, 8.4% ± 2.6%; *GFP*, 2.6% ± 1.1%), these levels were very low compared with those achieved by ionizable lipid-based LNPs with sgRNA delivery alone or *Cas9* mRNA + sgRNA formulations.[19,20] Interestingly, efficient *in vivo* editing using ionizable lipid-based LNPs required extra modifications on the sgRNA compared with the standard end-modified sgRNA chemical structure.[19] Using the design identified by Finn et al.,[19] here called ultra-modified sgRNA (Figure 2B), the *Npc1*-targeting sgRNA was synthesized using these

enhanced modifications and reformulated at a 1.2 mg/mL loading concentration using INVFT3.0 for comparison of i.v. versus intraperitoneal (i.p.) systemic delivery routes. Using i.p. administration, on average, 21% ± 5.3% editing was achieved in the liver, and these results were comparable with i.v. injection (17% ± 7.2%) when groups were dosed equally at 0.75 mg/kg (sgRNA weight (wt)/mouse wt) (Figure 2C). To increase editing efficiencies in the liver, we decided to increase the dose volume as opposed to loading higher concentrations of sgRNA in a fixed dose volume because liver editing using sgRNA loading concentrations of 1 mg/mL or 2 mg/mL were comparable (Figure 2A). Because i.p. administration can tolerate higher volumes of dosing solutions at more repetitive frequencies, we reasoned that this route offered the most flexibility to optimize *in vivo* editing efficacy. In addition to the higher dose potential of the i.p. route, the efficacy of standard end-modified versus ultra-modified sgRNAs was compared directly. *Cas9*$^{tg/tg}$ mice dosed i.p. at 1.5 mg/kg with sgRNA-INVFT3.0 formulations increased the average editing percentage in the liver from 21% ± 4.8% using end-modified sgRNA to 51% ± 5.2% using ultra-modified sgRNA (Figure 2D).

Although the LOF indels reported here and throughout the manuscript are based on Sanger sequencing using Synthego Inference of CRISPR Edits (ICE) (Materials and methods), the frequencies compared with amplicon sequencing using next-generation sequencing (NGS) techniques highlighted a slight underestimation because ultra-modified sgRNA-generated indels scored by Sanger sequencing reported 53% for one data point, and NGS indicated 62% indel formation for the same sample (Figure 2E). These differences were also detected from cell line-edited samples (Figure S1D). Because of the speed and reasonable reliability to detect high-frequency indels provided by decomposition of Sanger sequencing, we continued to use this method for the remainder of the study with acceptance of potential under-representation of the actual editing events (Figures 2E and S1D). INVFT3.0 provided an uncomplicated method for rapidly assessing ultra-modified sgRNA efficiencies *in vivo* with reproducible indel frequencies of greater than 50% using a single dose in *Cas9*$^{tg/tg}$ mice. Because these reagents and mice are commercially readily available, *in vitro* studies can transition to pre-clinical testing in an expedited manner.

Immunocompromised Ifnar1 knockout mice and those crossed with Cas9$^{tg/tg}$ mice serve as lethal models for VSV-EBOV

Various mouse models have been developed for EBOV, and common models use mouse-adapted EBOV (MA-EBOV) strains.[1,21] Mouse adaptation is required for infection of WT immunocompetent mice because these mice are resistant to WT or primary isolate EBOV infection. MA-EBOV causes uniform mortality between days 7–9 with an infection characterized by extensive viremia and disease pathogenesis of the endoreticular organs of the liver and spleen.[21] Although adapted for lethal disease in mice, MA-EBOV strains still require biosafety level 4 (BSL-4) containment for handling. Replication-competent VSV-EBOV is a BSL-2 virus that mimics viral entry and fusion of authentic EBOV and has been useful for *in vitro* studies that include discovery and characterization of EBOV countermeasures. VSV-EBOV is also a vaccine that provides complete protection to lethal EBOV challenge in immunocompetent mice.[22] In immunocompromised mice such as those with STAT1 deficiency, VSV-EBOV causes lethal disease.[23] Because the *Ifnar1* knockout mouse is a common model for many viruses that do not cause disease in immunocompetent mice, including WT EBOV strains, and is now available more readily from commercial vendors, we began VSV-EBOV mouse model development under animal biosafety level 2 (ABSL-2) containment by verifying the lethal dose in IFNAR1 knockout (KO) mice.

Ifnar1$^{-/-}$ mice were challenged with VSV-EBOV lacking the GFP reporter through i.p. administration in a six-point, 10-fold dilution series starting with 10^7 plaque-forming units (PFUs) (Figure 3A). All challenge doses resulted in uniform lethality, with mice succumbing to disease within 2–3 days of infection for the higher doses and 3–4 days for the lower doses. To characterize the tissue tropism of VSV-EBOV infection in *Ifnar1*$^{-/-}$ mice using a 100 PFU dose, groups of infected mice were euthanized 24 h post-infection (hpi), 48 hpi, or 72 hpi and the liver, spleen, and serum were analyzed for virus titers (Figure 3B). Onset of infection in these individuals was rapid and reached 10^6–10^7 PFU per gram of tissue or per milliliter of serum by 48 hpi. The kinetics and titers of virus dissemination in *Ifnar1*$^{-/-}$ mice closely resembled the tropism of MA-EBOV in WT mice, suggesting that Npc1-dependent entry in mice dictates the tissue targets.[21] Considering the parallel of VSV-EBOV and MA-EBOV animal models, we continued to develop this model with the goal of enabling rapid *in vivo* characterization of host factor involvement in the pathogenesis of EBOV by crossing *Cas9* transgenic mice with *Ifnar1*$^{-/-}$ mice.

When a cohort of double-homozygous *Cas9* $^{tg/tg}$; *Ifnar1* $^{-/-}$ mice was available, they were infected i.p. with VSV-EBOV using 100 PFUs to assess the survival profile compared with *Ifnar1*$^{-/-}$ mice (Figure 3C). Introduction of the *Cas9* transgene allele into *Ifnar1*$^{-/-}$ mice did not alter their survival pattern compared with *Ifnar1*$^{-/-}$ mice because lethal disease occurred similarly between days 3–4 after infection with VSV-EBOV. At the endpoint of this study, liver and spleen tissues were dissected for histological analysis and assessment of the presence of viral antigen (Figures 3D and 3E). Severe tissue necrosis was apparent in the liver of VSV-EBOV-infected mice by day 3, and viral replication in liver and spleen tissues was also abundant, as indicated by immunohistochemistry staining of the EBOV glycoprotein. Therefore, *Cas9*$^{tg/tg}$; *Ifnar1*$^{-/-}$ mice can serve as a versatile ABSL-2 model for rapid characterization of genetic factors affecting entry of EBOV *in vivo*.

Multi-dosing of sgRNA LNPs in Cas9$^{tg/tg}$; Ifnar1$^{-/-}$ mice results in liver-specific cumulative editing

As shown previously in *Cas9*$^{tg/tg}$ mice, we were able to achieve 51% ± 5.2% editing at the *Npc1* locus with a single dose of ultra-modified sgRNA using INVFT3.0. Although these editing levels could potentially provide complete or partial protection against VSV-EBOV challenge, we sought to maximize levels of LOF editing before commencing *in vivo* efficacy studies. To reach these *in vivo* LOF

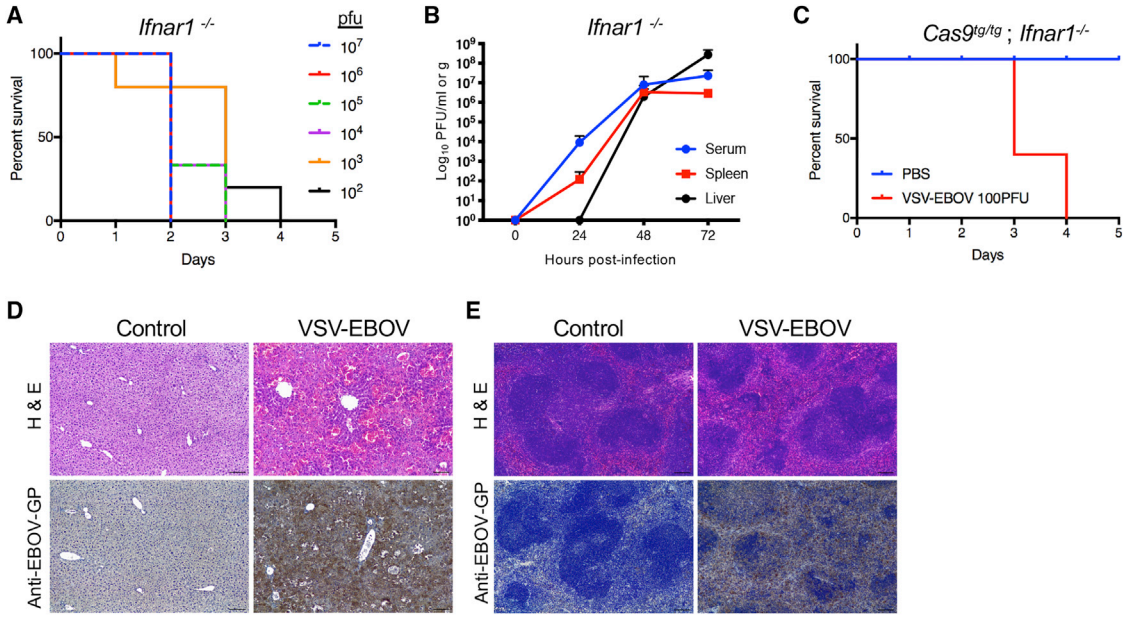

Figure 3. Immunocompromised IFNAR1 KO mice and those crossed with *Cas9* transgenic mice serve as lethal models for VSV-EBOV

(A) IFN alpha receptor KO (*Ifnar1*$^{-/-}$) mice were challenged with VSV-EBOV through i.p. administration in a six-point, 10-fold dilution series starting with 10^7 plaque forming units (PFUs). Survival curves are shown with 5 mice per challenge dose. (B) A time course experiment of VSV-EBOV tissue and blood dissemination was performed using a challenge dose of 100 PFUs. Virus titers from tissues (PFUs/g) or serum (PFUs/mL) of three mice per time point are depicted as mean + standard deviation. (C) *Cas9* transgenic mice crossed with IFNAR1 KO mice (*Cas9*$^{tg/tg}$; *Ifnar1*$^{-/-}$) were challenged with VSV-EBOV or mock infected (PBS), and survival was measured. (D and E) Liver (D) and spleen (E) tissues were harvested on day 3 after infection with VSV-EBOV in *Cas9*$^{tg/tg}$; *Ifnar1*$^{-/-}$ mice and subjected to histological analysis via hematoxylin and eosin (H&E) staining or immunohistochemistry using antibodies against the Ebola glycoprotein (anti-EBOV-GP). Tissues from infected *Cas9*$^{tg/tg}$; *Ifnar1*$^{-/-}$ mice were compared with control (PBS)-treated mice. Scale bars, 100 μm.

editing thresholds, *Cas9*$^{tg/tg}$; *Ifnar1*$^{-/-}$ mice were given a multi-dose treatment of *Npc1* sgRNA LNPs at low (0.75 mg/kg) and high (1.5 mg/kg) concentrations, which were compared with single-dose regimens (Figure 4A). Multi-dose treatments consisted of two doses given 7 days apart, and liver editing percentages were analyzed synchronously between single- and double-dosed mice 14 days after the first dose. Cumulative editing occurred under low- and high-dose conditions, and editing increased on average from 28.5% ± 12.3% to 39.8% ± 13.6% in the 0.75 mg/kg treatment groups and from 50.8% ± 16% to 73.5% ± 5% in the 1.5 mg/kg dose groups when comparing single- versus double-dose treatments, respectively. Interestingly, variability in editing percentages under the high double dose condition was minimal and less than half of all other conditions tested. This result suggested that we achieved consistency and reproducibility by maximizing the performance of the formulation. The LOF indel frequencies of high-dose-treated mice were then analyzed in additional tissues, and these studies revealed liver-specific editing of sgRNAs delivered using INVFT3.0 because the spleen, kidneys, or lungs were not edited (Figure 4B). I.P. delivery coupled with the LNP sizes associated specifically with sgRNA cargo could influence the liver-only editing effect.

To validate functional reduction of Npc1 protein expression in sgRNA LNP-dosed mice, liver of mice with approximately 0%, 25%, or 50% editing in the liver were subjected to western blot analysis (Figure 4C). These western blots indicated that, with 50% editing at the *Npc1* locus, we observed relatively undetectable levels of Npc1 protein in liver homogenates of *Cas9*$^{tg/tg}$; *Ifnar1*$^{-/-}$ mice. Last, histological analysis from tissues of high-double-dosed *Npc1*-sgRNA-treated mice revealed no apparent gross anatomical changes compared with controls within 14 days after the first dose (Figure 4D). Multi-dosing sgRNA delivery with INVFT3.0 provided high levels of liver-specific LOF editing at the *Npc1* locus in immunocompromised *Cas9* transgenic mice.

Liver-specific editing of Npc1 in Cas9$^{tg/tg}$; Ifnar1$^{-/-}$ mice provides complete protection against lethal VSV-EBOV challenge

Previous studies of EBOV infection in mice carrying *Npc1* homozygous or heterozygous mutations have demonstrated a strong role of systemic *Npc1* expression as a determinant of EBOV pathogenesis because *Npc1*$^{-/-}$ mice were completely protected from lethal EBOV infection, and 90% of *Npc1*$^{+/-}$ mice were also protected.[24] However, the role of particular tissues in EBOV disease progression is not fully understood. These types of studies can be assessed using conditional KO mutant mice or now more rapidly using CRISPR technology. Using our optimized liver-specific editing in mice using INVFT3.0, *Npc1*-edited *Cas9*$^{tg/tg}$; *Ifnar1*$^{-/-}$ mice that received double-dose sgRNA treatments using i.p. delivery were infected i.p. with VSV-EBOV 7 days after the second sgRNA dose (Figure 5A).

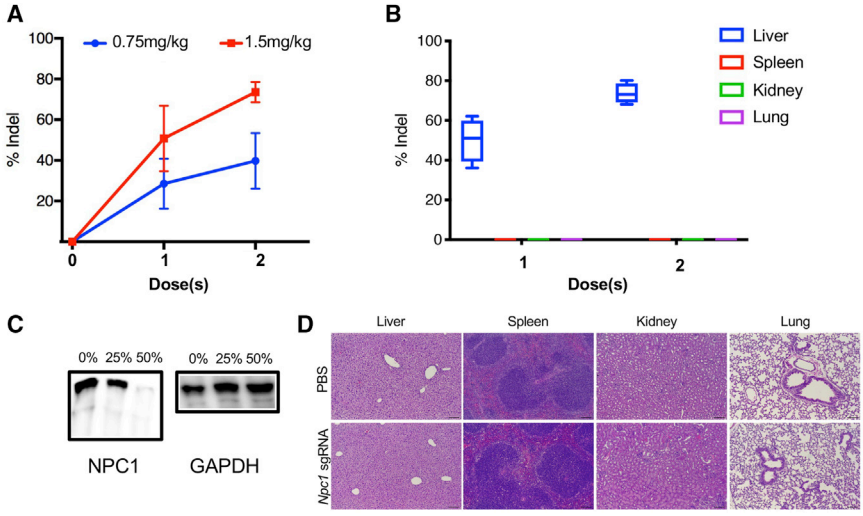

Figure 4. Multi-dosing of sgRNA LNPs in *Cas9*$^{tg/tg}$; *Ifnar1*$^{-/-}$ mice results in liver-specific cumulative editing

(A) INVFT3.0 LNPs were loaded with ultra-modified sgRNA targeting NPC1 and administered to immunocompromised Cas9 transgenic mice (*Cas9*$^{tg/tg}$; *Ifnar1*$^{-/-}$) via i.p. injection at 0.75 mg/kg or 1.5 mg/kg doses. Another equivalent dose was given to a subset of mice 7 days after the first dose. All mice were subjected to indel analysis of liver tissue on day 14 after the first dose. Data points are average of 4 mice per group ± standard deviation. (B) Percent indels from other tissues in addition to liver are shown for the 1.5 mg/kg dosing condition (n = 4). (N.D., not detected). (C) NPC1 protein expression from liver homogenates of mice edited at the *Npc1* locus at 0% (PBS), 25%, or 50% were analyzed using western blots. GAPDH was used as a loading control. (D) Histological analysis via H&E staining was performed on tissues harvested from Npc1 sgRNA LNP-treated (double dose, 1.5 mg/kg) mice along with controls (PBS treated). Representative images are shown. Scale bars, 100 μm.

As controls, mice dosed with PBS and non-targeting sgRNAs formulated using INVFT3.0 were infected similarly with VSV-EBOV. As expected, VSV-EBOV infection in both control groups led to uniform lethality by day 3 after infection, but, interestingly, *Npc1* sgRNA-treated mice were completely protected from lethal VSV-EBOV challenge. According to daily weight measurements of *Npc1*-edited mice, most mice initially lost weight between days 5–8 after infection before recovering and gaining weight (Figure 5B). These data indicated that, although liver-specific editing protected mice from severe disease, it was unable to completely prevent symptomatic infection, perhaps because of early infection outside of the liver. Virus replication (Figure 5C) and *Npc1* editing levels (Figure 5D) in the liver and spleen were examined at the end of the study and compared with control mice dosed with non-targeting sgRNA that succumbed to disease. Viral RNA copies in the tissues of control mice, on average, were 3.7×10^4 in the liver and 4.9×10^3 in the spleen, whereas viral RNA copies in *Npc1*-edited mice were 11.2 in the liver and 3.5 in the spleen. The final *Npc1* editing levels in *Cas9*$^{tg/tg}$; *Ifnar1*$^{-/-}$ mice on day 28 after the initial sgRNA dose was 62% ± 6.4%, suggesting that editing was stable and maintained during the infection study. These results suggest that safe prophylactic therapeutic agents targeting Npc1 in the liver could provide efficient protection against EBOV infection.

DISCUSSION

In this study, we demonstrated facile methods that enable highly efficient genome editing in the liver of *Cas9*$^{tg/tg}$ mice and those crossed with IFNAR1 KO mice. Although these techniques are useful for a variety of applications involving diseases affecting the liver, we highlight their utility for studying host factors involved in highly pathogenic virus infection. By targeting *Npc1* for LOF in the liver using INVFT3.0-based CRISPR sgRNA delivery, mice survived lethal infection in a surrogate BSL-2 EBOV model that mimics the tissue tropism of the BSL-4 MA-EBOV model.[21] These results extend the current understanding of NPC1 function in EBOV pathogenesis. Systemic KO and knockdown of *Npc1* obtained through homozygous or heterozygous mutations, respectively, have been shown to protect against lethal EBOV challenge to levels of 90% or greater.[24] However, our results indicate that the liver may serve as the most critical organ involved in EBOV pathogenesis in mouse models because liver-specific partial KO of *Npc1* resulted in complete protection against replication-competent Ebola pseudovirus lethality. Duplicating these studies using WT or MA EBOV in *Cas9*$^{tg/tg}$; *Ifnar1*$^{-/-}$ or *Cas9*$^{tg/tg}$ mice, respectively, would ultimately confirm these findings, but the data as shown provide evidence for continued investigation of prophylactic treatments targeted to the liver by traditional or novel means against EBOV.

Because the parameters are now optimized for rapid genome editing in the liver of *Cas9*$^{tg/tg}$ and *Cas9*$^{tg/tg}$; *Ifnar1*$^{-/-}$ mice, other host factor genes can be screened rapidly *in vivo* using these commercially available reagents. To continue screening host factors *in vivo* using the methods and models described here, additional factors would be limited to those that facilitate virus entry because of the limitations of a VSV-based surrogate virus infection model. A number of host genes involved in EBOV attachment and fusion have been described over the years,[13,25,26] but more recently, CRISPR KO screening against WT EBOV conducted under BSL-4 containment has identified novel entry factors that await *in vivo* validation.[27]

The *Cas9*$^{tg/tg}$; *Ifnar1*$^{-/-}$ model for genome editing of host factors could easily extend to other viruses of pandemic potential.[4] For instance, Rift Valley fever virus (RVFV) is a category A high-priority pathogen listed as a biodefense threat alongside EBOV that causes mainly hepatic disease in animal models.[28] WT RVFV studies are conducted under BSL-3 containment, but studies with the vaccine strain MP-12 are performed under BSL-2

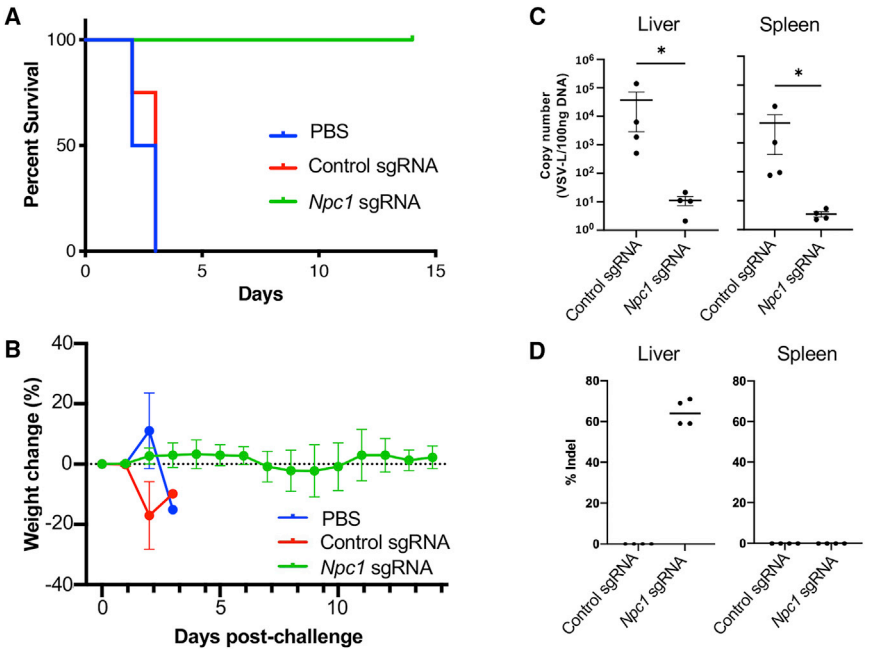

Figure 5. Liver-specific editing of *Npc1* in *Cas9*$^{tg/tg}$; *Ifnar1*$^{-/-}$ mice provides complete protection against lethal VSV-EBOV challenge

(A) *Cas9*$^{tg/tg}$; *Ifnar1*$^{-/-}$ mice were dosed twice at a 7-day interval with *Npc1* targeting sgRNA LNPs or controls that included PBS or non-targeting sgRNA LNPs and subsequently challenged with VSV-EBOV 7 days after the second dose (n = 4 per group). (B) Survival was measured for 14 days after challenge, and the weights of the PBS- or sgRNA LNP-treated groups were recorded daily and averaged as percent change from day 0. Individual mouse weights are represented in different colors. (C and D) Copies of the VSV polymerase gene (L) measured by qRT-PCR (C) and editing at the *Npc1* locus measured using indel analysis (D) from tissues collected at the endpoint of the study for *Npc1* sgRNA-treated mice or mice that succumbed to disease under the control sgRNA LNP condition. Data are depicted as mean ± standard deviation. *p < 0.05.

containment.[29] RVFV-MP-12 causes lethal disease in *Ifnar1*$^{-/-}$ mice;[30] therefore, INVFT3.0-mediated, liver-specific genome editing could be used for *in vivo* screening of host factors involved in RVFV infection and pathogenesis. Beyond EBOV and RVFV, IFNAR KO mice have been useful in animal model studies involving a diverse set of filoviruses, bunyaviruses, flaviviruses, alphaviruses, and henipaviruses, facilitating use of *Cas9*$^{tg/tg}$; *Ifnar1*$^{-/-}$ mice for rapid characterization of host factors for many threats with pandemic potential.[3]

Last, although INVFT3.0 was originally developed for efficient delivery of siRNA to the liver of mice, other studies have expanded their versatility by using localized delivery methods to the brain, retina, and other regions.[31–33] Given the similarities between sgRNA and siRNA delivery to the liver using INVFT3.0, it is reasonable to conclude that the optimized sgRNA delivery formulations reported here could also edit tissues outside of the liver for further characterization of non-hepatic tissue involvement in viral pathogenesis. *Cas9*$^{tg/tg}$; *Ifnar1*$^{-/-}$ mice can serve as an ABSL-2 model for rapid *in vivo* characterization of genetic factors affecting entry of EBOV and, by extension, can serve as a more general platform for characterization of host factors in disease pathogenesis and therapy development for many other emerging viruses.

MATERIALS AND METHODS

Cells, viruses, and reagents

All cell lines were maintained in culture medium supplemented with 10% fetal bovine serum (FBS) (15% FBS for LA4 cells), 100 g/mL penicillin, and 100 U/mL streptomycin (Thermo Fisher Scientific, Waltham, MA) at 37°C under 5% CO_2. LA4 (mouse lung epithelial) cells were cultured in Ham's F12K medium, Hepa1-6 (mouse hepatoma) cells were cultured in Dulbecco's modified Eagle's medium, IC-21 (mouse macrophage) cells were cultured in RPMI-1640 medium, and Vero (African green monkey kidney) cells were cultured in minimum essential medium alpha. The recombinant VSV expressing the Ebola glycoprotein (EBOV-GP) gene was derived from a full-length cDNA clone of VSV Indiana serotype 1, in which the VSV-G envelope protein has been replaced with EBOV-GP (VSV-EBOV). The EBOV-GP gene (GenBank: L11365) was cloned from a plasmid available from BEI Resources (Manassas, VA; catalog number NR-19814). VSV-EBOV-GFP was derived from the cDNA clone of VSV-EBOV, where the VSV-P gene contained an N-terminal fusion to GFP, and this reporter virus was only used for *in vitro* experiments. VSV-EBOV and VSV-EBOV-GFP were propagated in Vero cells, and virus titers were quantified by standard agarose overlay plaque assays. Antibodies used for western blot analysis included rabbit monoclonal anti-Npc1 (Abcam, Cambridge, MA; catalog number ab134113) and rabbit monoclonal anti-Gapdh (Cell Signaling Technology, Danvers, MA; catalog number 3683).

In vitro Npc1 sgRNA screening

sgRNAs targeting mouse *Npc1* were selected using publicly available design tools, and top-ranking sequences were cross-referenced to each other (Figure S1A). Three sequences were identified and synthesized as end-modified sgRNAs (Synthego, Redwood City, CA) (Table S1). sgRNAs were complexed with SpyCas9 protein (Integrated DNA Technologies, Coralville, IA) and transfected into LA4, Hepa1-6, or IC-21 cells using CRISPRmax (Thermo Fisher Scientific, Waltham, MA) according to the manufacturer's instructions. Transfected cells were subsequently subjected to phenotypic and indel editing analysis 4 days or longer after transfection.

Indel analysis

DNA from *Npc1* LOF-edited samples derived from cell cultures or mouse tissues were isolated and purified using the Blood and Tissue Genomic Mini-prep Kit (Epoch Life Science, Sugar Land, TX). PCR products encompassing the mouse *Npc1* editing site were amplified using primers listed in Table S1, column purified, and sent for Sanger sequencing (Genewiz, South San Francisco, CA). Chromatograph files from control and edited samples were analyzed by the sequence decomposition software Synthego ICE, which provided rapid and reliable assessment of indel profiles and frequencies from CRISPR editing experiments. Amplicon sequencing was also performed on a subset of *Npc1*-edited samples using NGS techniques. PCR products were amplified in two rounds, adding adaptor sequences and barcodes to the ends of the amplicons. Pooled PCR reactions were column purified and additionally gel purified. PCR product concentration and quality were assessed using the Qubit High-Sensitivity dsDNA Kit and a Bioanalyzer 2100 high-sensitivity chip (Agilent Technologies, Santa Clara, CA). NGS was performed on an Illumina (San Diego, CA) NextSeq using 500/550 Mid Output Kit v.2.5 (300 cycles) following the manufacturer's protocol. Raw amplicon data were analyzed for indels using the CRIS.py software.[34] The most prominent indel sequences and frequencies for each sample are highlighted in the figures and Supplemental information.

Cholesterol accumulation through filipin staining

LA4 cells with or without indels at the *Npc1* locus were fixed with 3% paraformaldehyde (PFA) for 1 h at room temperature (RT). After quenching free PFA with 1.5 mg glycine/mL in PBS for 10 min at RT, cells were stained with 0.05 mg/mL filipin (Sigma-Aldrich, St. Louis, MO; catalog number SAE0088) in PBS/10% FBS for 2 h at RT. Following the PBS wash, the cells were counterstained with the nuclear dye propidium iodide (PI) for 10 min at RT. For imaging and cell cytometry analysis, the CellInsight CX7 microscope platform was used with the standard excitation/emission wavelength for filipin and PI, respectively. Using the built-in cell cytometry analysis feature, the number of filipin-stained cells (surrogate for accumulated cholesterol) and total number of cells by counting PI-stained nuclei were determined. The percentage of filipin stained cells was determined by dividing the number of filipin stained cells by the total number of cells.

Cas9$^{tg/tg}$, Ifnar1$^{-/-}$ *and* Cas9$^{tg/tg}$; Ifnar1$^{-/-}$ mouse models

All animal work was conducted in accordance with protocols approved by the Lawrence Livermore National Laboratory (LLNL) Institution Animal Care and Use Committee. *Cas9*$^{tg/tg}$ mice (*Rosa26-Cas9* knockin on the *C57BL/6J* genetic background, B6J.129(Cg)-*Gt(ROSA)26Sor*$^{tm1.1(CAG-cas9*,-EGFP)Fezh/J}$; The Jackson Laboratory, Farmington, CT; catalog number 026179) and *Ifnar1*$^{-/-}$ mice (global *Ifnar1* KO on the *C57BL/6J* genetic background, B6(Cg)-*Ifnar1*$^{tm1.2Es/J}$; The Jackson Laboratory, Farmington, CT; catalog number 028288) were bred separately at LLNL and also mated to generate a double-homozygous mutant *Cas9*$^{tg/tg}$; *Ifnar1*$^{-/-}$ mouse strain. All experiments were performed with 6- to 10-week-old mice.

In vivo sgRNA delivery using INVFT3.0

CRISPR sgRNAs were encapsulated into INVFT3.0 LNPs originally designed for efficient *in vivo* delivery of siRNA. The manufacturer's protocol (Thermo Fisher Scientific, Waltham, MA) was modified slightly for sgRNA loading and delivery. Initially, standard end-modified sgRNAs purchased from Synthego (Redwood City, CA) were diluted to concentrations of 1 mg/mL or 2 mg/mL in distilled water (dH_2O), mixed with complexation buffer (CB) from the kit, and subsequently combined with INVFT3.0 at a volume ratio of 1:1:2 (sgRNA:CB:INVFT3.0). The solution was heated to 50°C for 30 min on a heat block, diluted 5-fold with PBS, and then administered i.v. via tail vein injection using 200 μL of sgRNA LNPs. For all other *in vivo* editing experiments, INVFT3.0 LNPs were formulated using an initial loading concentration of 1.2 mg/mL of end-modified or ultra-modified sgRNAs (Synthego, Redwood City, CA) (Figure 2B) using similar volume ratios and protocols as before, but the final dilution with PBS was 4-fold instead of 5-fold. LNP administration typically occurred within 1–2 h after formation and through i.p. injection at doses of 0.75 mg/kg (∼200 μL LNPs per 20-g mouse) or 1.5 mg/kg (∼400 μL LNPs per 20-g mouse). At the end of the study, mice were euthanized, and liver or liver, spleen, kidneys, and lungs were dissected from 3–4 animals per group.

Mouse model of VSV-EBOV infection

Ifnar1$^{-/-}$ mice were tested for their susceptibility to lethal disease by surrogate EBOV infection using VSV-EBOV. *Ifnar1*$^{-/-}$ mice were challenged with VSV-EBOV through i.p. administration in a six-point, 10-fold dilution series starting with 10^7 PFUs. All mice were maintained in positive airflow barrier housing under specific pathogen-free conditions. Animals were moved into negative airflow ABSL-2 containment housing 24 h prior to VSV-EBOV infection. Mice were observed at least daily and twice daily when symptomatic, with body condition scores and animal weights measured. Animals that reached the humane endpoint were euthanized. For time course experiments, four mice from each group (24 hpi, 48 hpi, or 72 hpi) were euthanized and dissected for liver, spleen, and serum. Organs were weighed and then homogenized using disposable tissue grinders, and tissue lysate was assessed for viral load using a standard plaque assay. The identified lethal dose of 100 PFUs of VSV-EBOV in IFNAR KO mice was then verified in *Cas9*$^{tg/tg}$; *Ifnar1*$^{-/-}$ mice. At the endpoint of the *Cas9*$^{tg/tg}$; *Ifnar1*$^{-/-}$ mouse study, tissues (liver and spleen) were dissected for histological analysis and assessment of the presence of viral antigen.

Histology and immunohistochemistry

Mouse tissues derived from liver, spleens, kidneys, and lungs were dissected and fixed in 4% PFA overnight. Dissected tissues were then transitioned into paraffin wax using an ASP300S tissue processor (Leica, Buffalo Grove, IL). Tissue samples were then embedded in paraffin blocks using a HistoCore Arcadia H embedder (Leica, Buffalo Grove, IL). Samples were cut to generate 5-μm sections and mounted on slides. Hematoxylin and eosin staining was performed manually in house. Stained slides were imaged using a Leica ICC50E camera and microscope at 40×, 100×, or 400× magnification. For

immunohistochemistry, tissues mounted on charged slides were deparaffinized, rehydrated through alcohol steps, and then treated with citrate buffer under high pressure (Cuisinart Pressure Cooker) for antigen retrieval. Following antigen retrieval, the slides were subjected to 3% hydrogen peroxide to inactivate endogenous peroxidases and blocked with 5% goat serum and 0.1% Triton X-100. The slides were incubated with a primary rabbit anti-EBOV-GP antibody (1:100) (IBT Bioservices, Rockville, MD) overnight at 4°C. The primary antibody was removed, samples were washed 5 times with PBS, and secondary goat anti-rabbit horseradish peroxidase (HRP) antibody (1:500) (Thermo Fisher Scientific, Waltham, MA) was then added. DAB substrate (3,3'-diaminobenzidine) reagent (SK-4100, Vector Laboratories, Burlingame, CA) was added to samples for 10 min for detection of HRP activity, and then the samples were washed with water. Mayer's hematoxylin (Sigma-Aldrich, St. Louis, MO) was used to counterstain for 8 min with subsequent water washes and stepwise dehydration with ethanol, and samples were finally coverslipped using Permount mounting medium. Stained slides were imaged on a Leica ICC50E camera and microscope at 40×, 100×, or 400× magnification.

Measurement of VSV-L gene copies

To extract RNA, mouse tissues were homogenized in RX tissue lysis buffer (GenCatch Total RNA Miniprep Kit, Epoch Life Science, Sugar Land, TX) using a handheld pestle motor. The resulting homogenate was clarified by centrifugation, and the RNA from the supernatant was isolated and purified using the GenCatch Total RNA Miniprep Kit (Epoch Life Science, Sugar Land, TX). Following extraction of RNA, cDNA was synthesized using the Superscript III First Strand Synthesis System (Thermo Fisher Scientific, Waltham, MA). Quantitative PCR reactions were set up in triplicate using Primetime Gene Expression Master Mix (IDT, Coralville, IA), 100 ng of cDNA, and a custom VSV-L primer and probe set (Table S1). Reactions were then performed on a Bio-Rad (Hercules, CA) CFX96 Touch real-time system, and data analysis for expression of VSV-L was carried out using a standard curve of VSV-L DNA.

Statistical analysis

All results where individual values were averaged were depicted as mean ± standard deviation. To determine significance, two-tailed t tests for the experiments in Figure 2 were performed. In Figure 5, for viral RNA copy number statistics, graphs were plotted in GraphPad Prism 9, and p values were calculated in Prism 9 using a Mann-Whitney test. $p < 0.05$ was considered significant and $p < 0.01$ very significant.

SUPPLEMENTAL INFORMATION

Supplemental information can be found online at https://doi.org/10.1016/j.omtm.2021.09.012.

ACKNOWLEDGMENTS

This work was supported by the Laboratory Directed Research and Development Program at Sandia National Laboratories (SNL) and the DARPA Safe Genes Program under contract HR0011-17-2-0043. SNL is a multi-mission laboratory managed and operated by National Technology & Engineering Solutions of Sandia, LLC, a wholly owned subsidiary of Honeywell International Inc., for the U.S. Department of Energy's National Nuclear Security Administration under contract DE-NA0003525. This paper describes objective technical results and analyses. Any subjective views or opinions that might be expressed in the paper do not necessarily represent the views of the U.S. Department of Energy or the United States Government. All work performed at Lawrence Livermore National Laboratory is performed under the auspices (LLNL-JRNL-821248) of the U.S. Department of Energy under contract DE-AC52-07NA27344. The authors gratefully acknowledge Richard Mosseso for CX7 imager training, Christine Thatcher for histology training, and Kimberly Butler for manuscript review.

AUTHOR CONTRIBUTIONS

N.C., P.D., S.J.L., E.A.S., J.L.S., A.S., and O.A.N. conducted experiments. N.C., P.D., S.J.L., E.A.S., J.L.S., and O.A.N. designed experiments and analyzed data. Y.L. implemented computer code and supporting algorithms. N.C. and O.N. wrote the original draft, and all authors provided review and editing. J.S.S. and O.N. provided project supervision and supported funding acquisition.

DECLARATION OF INTERESTS

The authors declare no competing interests.

REFERENCES

1. Bradfute, S.B., Warfield, K.L., and Bray, M. (2012). Mouse models for filovirus infections. Viruses *4*, 1477–1508.
2. Comer, J.E., Escaffre, O., Neef, N., Brasel, T., Juelich, T.L., Smith, J.K., Smith, J., Kalveram, B., Perez, D.D., Massey, S., et al. (2019). Filovirus Virulence in Interferon α/β and γ Double Knockout Mice, and Treatment with Favipiravir. Viruses *11*, 137.
3. Wong, G., and Qiu, X.G. (2018). Type I interferon receptor knockout mice as models for infection of highly pathogenic viruses with outbreak potential. Zool. Res. *39*, 3–14.
4. Marín-Lopez, A., Calvo-Pinilla, E., Moreno, S., Utrilla-Trigo, S., Nogales, A., Brun, A., Fikrig, E., and Ortego, J. (2019). Modeling Arboviral Infection in Mice Lacking the Interferon Alpha/Beta Receptor. Viruses *11*, 35.
5. Kaufmann, S.H.E., Dorhoi, A., Hotchkiss, R.S., and Bartenschlager, R. (2018). Host-directed therapies for bacterial and viral infections. Nat. Rev. Drug Discov. *17*, 35–56.
6. Puschnik, A.S., Majzoub, K., Ooi, Y.S., and Carette, J.E. (2017). A CRISPR toolbox to study virus-host interactions. Nat. Rev. Microbiol. *15*, 351–364.
7. Ramage, H., and Cherry, S. (2015). Virus-Host Interactions: From Unbiased Genetic Screens to Function. Annu. Rev. Virol. *2*, 497–524.
8. Knott, G.J., and Doudna, J.A. (2018). CRISPR-Cas guides the future of genetic engineering. Science *361*, 866–869.
9. Lino, C.A., Harper, J.C., Carney, J.P., and Timlin, J.A. (2018). Delivering CRISPR: a review of the challenges and approaches. Drug Deliv. *25*, 1234–1257.
10. Noureddine, A., Maestas-Olguin, A., Saada, E.A., LaBauve, A.E., Agola, J.O., Baty, K.E., Howard, T., Sabo, J.K., Espinoza, C.R.S., Doudna, J.A., et al. (2020). Engineering of monosized lipid-coated mesoporous silica nanoparticles for CRISPR delivery. Acta Biomater. *114*, 358–368.
11. Chuang, Y.F., Phipps, A.J., Lin, F.L., Hecht, V., Hewitt, A.W., Wang, P.Y., and Liu, G.S. (2021). Approach for in vivo delivery of CRISPR/Cas system: a recent update and future prospect. Cell. Mol. Life Sci. *78*, 2683–2708.

12. Eguchi, A., De Mollerat Du Jeu, X., Johnson, C.D., Nektaria, A., and Feldstein, A.E. (2016). Liver Bid suppression for treatment of fibrosis associated with non-alcoholic steatohepatitis. J. Hepatol. *64*, 699–707.

13. Carette, J.E., Raaben, M., Wong, A.C., Herbert, A.S., Obernosterer, G., Mulherkar, N., Kuehne, A.I., Kranzusch, P.J., Griffin, A.M., Ruthel, G., et al. (2011). Ebola virus entry requires the cholesterol transporter Niemann-Pick C1. Nature *477*, 340–343.

14. Wang, H., Shi, Y., Song, J., Qi, J., Lu, G., Yan, J., and Gao, G.F. (2016). Ebola Viral Glycoprotein Bound to Its Endosomal Receptor Niemann-Pick C1. Cell *164*, 258–268.

15. Yang, X.L., Tan, C.W., Anderson, D.E., Jiang, R.D., Li, B., Zhang, W., Zhu, Y., Lim, X.F., Zhou, P., Liu, X.L., et al. (2019). Characterization of a filovirus (Měnglà virus) from Rousettus bats in China. Nat. Microbiol. *4*, 390–395.

16. Ng, M., Ndungo, E., Kaczmarek, M.E., Herbert, A.S., Binger, T., Kuehne, A.I., Jangra, R.K., Hawkins, J.A., Gifford, R.J., Biswas, R., et al. (2015). Filovirus receptor NPC1 contributes to species-specific patterns of ebolavirus susceptibility in bats. eLife *4*, e11785.

17. Ding, Q., Strong, A., Patel, K.M., Ng, S.L., Gosis, B.S., Regan, S.N., Cowan, C.A., Rader, D.J., and Musunuru, K. (2014). Permanent alteration of PCSK9 with in vivo CRISPR-Cas9 genome editing. Circ. Res. *115*, 488–492.

18. Watters, K.E., Fellmann, C., Bai, H.B., Ren, S.M., and Doudna, J.A. (2018). Systematic discovery of natural CRISPR-Cas12a inhibitors. Science *362*, 236–239.

19. Finn, J.D., Smith, A.R., Patel, M.C., Shaw, L., Youniss, M.R., van Heteren, J., Dirstine, T., Ciullo, C., Lescarbeau, R., Seitzer, J., et al. (2018). A Single Administration of CRISPR/Cas9 Lipid Nanoparticles Achieves Robust and Persistent In Vivo Genome Editing. Cell Rep. *22*, 2227–2235.

20. Yin, H., Song, C.Q., Suresh, S., Wu, Q., Walsh, S., Rhym, L.H., Mintzer, E., Bolukbasi, M.F., Zhu, L.J., Kauffman, K., et al. (2017). Structure-guided chemical modification of guide RNA enables potent non-viral in vivo genome editing. Nat. Biotechnol. *35*, 1179–1187.

21. Bray, M., Davis, K., Geisbert, T., Schmaljohn, C., and Huggins, J. (1998). A mouse model for evaluation of prophylaxis and therapy of Ebola hemorrhagic fever. J. Infect. Dis. *178*, 651–661.

22. Jones, S.M., Stroher, U., Fernando, L., Qiu, X., Alimonti, J., Melito, P., Bray, M., Klenk, H.D., and Feldmann, H. (2007). Assessment of a vesicular stomatitis virus-based vaccine by use of the mouse model of Ebola virus hemorrhagic fever. J. Infect. Dis. *196* (*Suppl 2*), S404–S412.

23. Marzi, A., Kercher, L., Marceau, J., York, A., Callsion, J., Gardner, D.J., Geisbert, T.W., and Feldmann, H. (2015). Stat1-Deficient Mice Are Not an Appropriate Model for Efficacy Testing of Recombinant Vesicular Stomatitis Virus-Based Filovirus Vaccines. J. Infect. Dis. *212* (*Suppl 2*), S404–S409.

24. Herbert, A.S., Davidson, C., Kuehne, A.I., Bakken, R., Braigen, S.Z., Gunn, K.E., Whelan, S.P., Brummelkamp, T.R., Twenhafel, N.A., Chandran, K., et al. (2015). Niemann-pick C1 is essential for ebolavirus replication and pathogenesis in vivo. MBio *6*, e00565–e15.

25. Moller-Tank, S., and Maury, W. (2015). Ebola virus entry: a curious and complex series of events. PLoS Pathog. *11*, e1004731.

26. Kang, Y.L., Chou, Y.Y., Rothlauf, P.W., Liu, Z., Soh, T.K., Cureton, D., Case, J.B., Chen, R.E., Diamond, M.S., Whelan, S.P.J., and Kirchhausen, T. (2020). Inhibition of PIKfyve kinase prevents infection by Zaire ebolavirus and SARS-CoV-2. Proc. Natl. Acad. Sci. USA *117*, 20803–20813.

27. Flint, M., Chatterjee, P., Lin, D.L., McMullan, L.K., Shrivastava-Ranjan, P., Bergeron, É., Lo, M.K., Welch, S.R., Nichol, S.T., Tai, A.W., and Spiropoulou, C.F. (2019). A genome-wide CRISPR screen identifies N-acetylglucosamine-1-phosphate transferase as a potential antiviral target for Ebola virus. Nat. Commun. *10*, 285.

28. Smith, D.R., Steele, K.E., Shamblin, J., Honko, A., Johnson, J., Reed, C., Kennedy, M., Chapman, J.L., and Hensley, L.E. (2010). The pathogenesis of Rift Valley fever virus in the mouse model. Virology *407*, 256–267.

29. Harmon, B., Schudel, B.R., Maar, D., Kozina, C., Ikegami, T., Tseng, C.T., and Negrete, O.A. (2012). Rift Valley fever virus strain MP-12 enters mammalian host cells via caveola-mediated endocytosis. J. Virol. *86*, 12954–12970.

30. Lorenzo, G., Martín-Folgar, R., Hevia, E., Boshra, H., and Brun, A. (2010). Protection against lethal Rift Valley fever virus (RVFV) infection in transgenic IFNAR(-/-) mice induced by different DNA vaccination regimens. Vaccine *28*, 2937–2944.

31. Chu-Tan, J.A., Fernando, N., Aggio-Bruce, R., Cioanca, A.V., Valter, K., Andronikou, N., deMollerat du Jeu, X., Rutar, M., Provis, J., and Natoli, R. (2020). A method for gene knockdown in the retina using a lipid-based carrier. Mol. Vis. *26*, 48–63.

32. Mokuda, S., Nakamichi, R., Matsuzaki, T., Ito, Y., Sato, T., Miyata, K., Inui, M., Olmer, M., Sugiyama, E., Lotz, M., and Asahara, H. (2019). Wwp2 maintains cartilage homeostasis through regulation of Adamts5. Nat. Commun. *10*, 2429.

33. Tanida, M., Yamamoto, N., Shibamoto, T., and Rahmouni, K. (2013). Involvement of hypothalamic AMP-activated protein kinase in leptin-induced sympathetic nerve activation. PLoS ONE *8*, e56660.

34. Connelly, J.P., and Pruett-Miller, S.M. (2019). CRIS.py: A Versatile and High-throughput Analysis Program for CRISPR-based Genome Editing. Sci. Rep. *9*, 4194.